ELSEVIER

Earth and Planetary Science Letters 160 (1998) 163–178

EPSL

Miocene seawater $^{187}Os/^{188}Os$ ratios inferred from metalliferous carbonates

Douglas N. Reusch [a], Greg Ravizza [b], Kirk A. Maasch [a,*], James D. Wright [a]

[a] *University of Maine, Department of Geological Sciences, Orono, ME 04469, USA*
[b] *Woods Hole Oceanographic Institute, Woods Hole, MA 02543, USA*

Received 25 August 1997; accepted 3 May 1998

Abstract

Seawater $^{187}Os/^{188}Os$ ratios for the Middle Miocene were reconstructed by measuring the $^{187}Os/^{188}Os$ ratios of metalliferous carbonates from the Pacific (DSDP 598) and Atlantic (DSDP 521) oceans. Atlantic and Pacific $^{187}Os/^{188}Os$ measurements are nearly indistinguishable and are consistent with previously published Os isotope records from Pacific cores. The Atlantic data reported here provide the first direct evidence that the long-term sedimentary $^{187}Os/^{188}Os$ record reflects whole-ocean changes in the Os isotopic composition of seawater. The Pacific and the Atlantic Os measurements confirm a long-term 0.01/Myr increase in marine $^{187}Os/^{188}Os$ ratios that began no later than 16 Ma. The beginning of the Os isotopic increase coincided with a decrease in the rate of increase of marine $^{87}Sr/^{86}Sr$ ratios at 16 Ma. A large increase of 1‰ in benthic foraminiferal $\delta^{18}O$ values, interpreted to reflect global cooling and ice sheet growth, began approximately 1 million years later at 14.8 Ma, and the long-term shift toward lower bulk carbonate $\delta^{13}C$ values began more than 2 Myr later around 13.6 Ma. The post-16 Ma increase in marine $^{187}Os/^{188}Os$ ratios was most likely forced by weathering of radiogenic materials, either old sediments or sialic crust with a sedimentary protolith. We consider two possible Miocene-specific geologic events that can account for both this increase in marine $^{187}Os/^{188}Os$ ratios and also nearly constant $^{87}Sr/^{86}Sr$ ratios: (1) the first glacial erosion of sediment-covered cratons in the Northern Hemisphere; (2) the exhumation of the Australian passive margin–New Guinea arc system. The latter event offers a mechanism, via enhanced availability of soluble Ca and Mg silicates in the arc terrane, for the maintenance of assumed low CO_2 levels after 15 Ma. The temporal resolution (three samples/Myr) of the $^{187}Os/^{188}Os$ record from Site 598, for which a stable isotope stratigraphy was also constructed, is significantly higher than that of previously published records. These high resolution data suggest oscillations with amplitudes of 0.01 to 0.02 and periods of around 1 Myr. Although variations in the $^{187}Os/^{188}Os$ record of this magnitude can be easily resolved analytically, this higher frequency signal must be verified at other sites before it can be safely interpreted as global in extent. However, the short-term $^{187}Os/^{188}Os$ variations may correlate inversely with short-term benthic foraminiferal $\delta^{18}O$ and bulk carbonate $\delta^{13}C$ variations that reflect glacioeustatic events.

Keywords: osmium; sea water; weathering; global change; Miocene

* Corresponding author. E-mail: kirk@iceage.umeqs.maine.edu

0012-821X/98/$19.00
PII S0012-821X(98)00082-X

1. Introduction

The effects of tectonic variables on climate have been a matter of interest since Chamberlin [1], noting a correlation between ice ages and orogenies, hypothesized a link between increased availability of silicates for weathering and decreased partial pressure of carbon dioxide (pCO_2). The gross features of the global carbon cycle are not a matter of contention. Carbon dioxide enters the atmosphere as a product of thermal degassing reactions and weathering of organic matter; it leaves the atmosphere via burial of carbonate, with Ca and Mg supplied by silicate weathering, and burial of organic matter [2]. Current work focuses upon establishing the feedbacks between climate, atmospheric (pCO_2), and C sources and burial fluxes, with an ultimate goal of understanding the natural processes which regulate Earth's climate system. The many proposed scenarios linking the C cycle and climate [3–7] demonstrate that these feedbacks remain poorly understood.

The marine $^{87}Sr/^{86}Sr$ and $^{187}Os/^{188}Os$ records are relevant to C cycle models because seawater ratios respond to changes in either the fluxes or the isotopic compositions of solutes delivered to the ocean. The marine $^{87}Sr/^{86}Sr$ record is commonly used to constrain the fluxes of these solutes [8,9]. Variations in the $^{87}Sr/^{86}Sr$ composition of seawater over geologic time are influenced by silicate and carbonate weathering, dissolution of marine carbonates, and ridge hydrothermal circulation [10], linking the Sr record to the inorganic C cycle. The marine $^{187}Os/^{188}Os$ record provides new and independent constraints on inputs to the ocean and the C cycle. Changes in the $^{187}Os/^{188}Os$ composition of seawater are related to the organic C cycle [11,12] and possibly silicate weathering [12,13], but are not influenced by the weathering of carbonates. Thus comparing and contrasting the $^{87}Sr/^{86}Sr$ and $^{187}Os/^{188}Os$ records should provide new insights into the climate–C cycle problem because these two tracers are linked to the C cycle in very different ways.

Benthic foraminiferal $\delta^{18}O$ values (Fig. 1a) increased by more than 1‰ during the Middle Miocene, reflecting cooling of bottom waters and expansion of ice sheets [14,15]. During this interval, the marine $^{87}Sr/^{86}Sr$ record exhibits a plateau in $^{87}Sr/^{86}Sr$ [6,16,17], while $^{187}Os/^{188}Os$ ratios (Fig. 1b) show an increasing trend that continues through the remainder of the Neogene [11,18]. Precise knowledge of the relative timing of these changes should help in determining their causes and mutual relationships. This study was designed to: (1) determine whether Atlantic (Deep Sea Drilling Project Site 521) and Pacific (Site 598) metalliferous sediments preserve similar records of Miocene Os isotopic variations on million year time scales; (2) provide an improved stratigraphic framework for Site 598, allowing a more reliable comparison with Middle Miocene records from other sites; and (3) determine if short-period oscillations (10^4–10^6 yr) are present in the $^{187}Os/^{188}Os$ record which are not captured in the $^{87}Sr/^{86}Sr$ record because of its long oceanic residence time (2×10^6 yr, [10]) compared to that of Os (10^4–10^5 yr, [13,19,20]). In addition, Reusch and Maasch [21] hypothesized that the Middle Miocene plateau in $^{87}Sr/^{86}Sr$ reflects the emergence of a nonradiogenic young volcanic source following the collision between the New Guinea arc and Australian passive margin. This scenario also predicts increases in the supplies of both nonradiogenic Os from Os-rich ultramafic material and radiogenic Os from the Australian margin exhumed during this collision.

2. Samples

Metalliferous carbonates rich in hydrothermal Fe and Mn oxides, derived from 'plume fall-out' as defined in German et al. [22], were chosen for this study. The dominant species of Os in seawater is thought to be the oxyanion $H_3OsO_6^-$ [23], which is scavenged by Fe and Mn oxides in hydrothermal plumes [24]. Previous work has demonstrated that these deposits record past changes in the Os isotopic composition of seawater on million year time scales [11]. Osmium isotopic analyses of bulk sediments and sediment leachates yield nearly indistinguishable results indicating that the vast majority of Os in these sediments is derived from seawater [18]. Although metalliferous sediments are genetically linked to sea-floor hydrothermal processes, plume fall-out deposits accumulating within 100 m of an active sea-floor hydrothermal system show no evidence of nonradiogenic mantle Os derived from

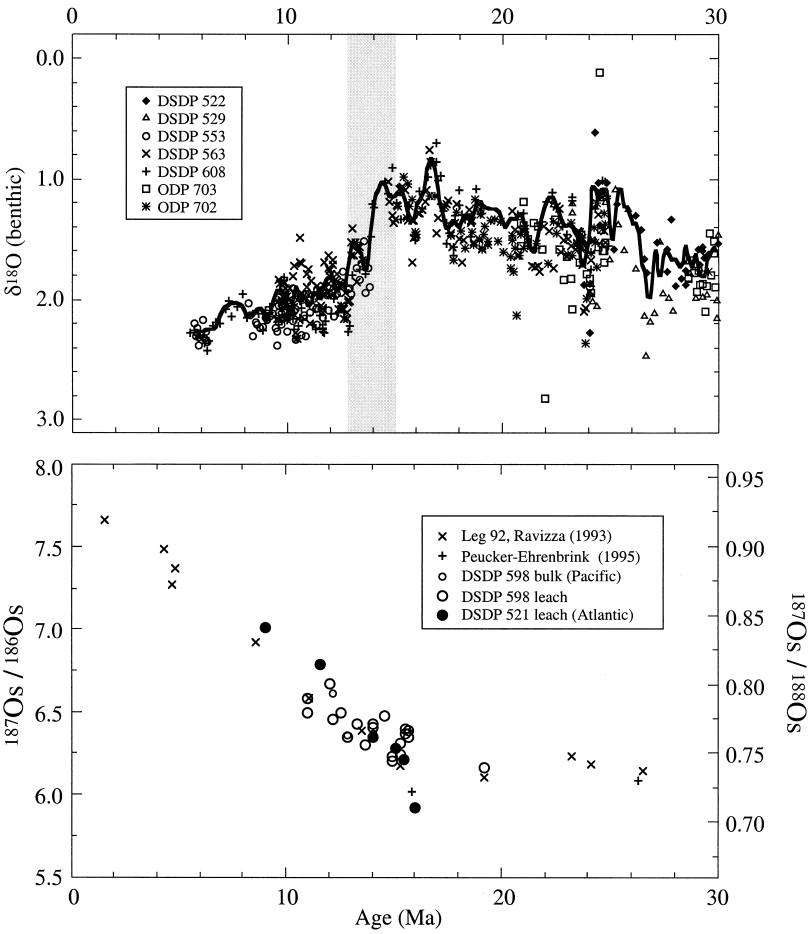

Fig. 1. (a) Benthic foraminiferal $\delta^{18}O$ record, 30–5 Ma [18]. Vertical shaded bar shows major $\delta^{18}O$ increase in the Middle Miocene. Dark line shows Mi $\delta^{18}O$ maxima [42,43] discussed in text, e.g. Mi2 (16 Ma), Mi2a (15 Ma), Mi3 (13.6 Ma), and Mi4 (12.8 Ma). (b) Temporal variations in the $^{187}Os/^{188}Os$ ratio of seawater inferred from analyses of metalliferous carbonates. The agreement of new measurements (circles) with previous measurements is good. Also, for Middle Miocene samples, the Atlantic measurements (solid circles) are indistinguishable from Pacific measurements. Note that the $^{187}Os/^{188}Os$ ratio is nearly constant before 16 Ma and increases at a rate of $0.1/10^6$ yr after 16 Ma.

sea-floor alteration, and appear to accurately record the $^{187}Os/^{188}Os$ composition of present-day seawater [25].

Metalliferous carbonates accumulate at rates on the order of 10 mm/10^3 yr, and contain planktonic foraminifera and nannofossils essential for correlating the marine $^{187}Os/^{188}Os$ record with other paleoceanographic records. These attributes of metalliferous carbonates afford the possibility of capturing the high frequency fluctuations in the seawater $^{187}Os/^{188}Os$ record that are expected based on residence time estimates. Pelagic clays [12,18] and Mn crusts [26] have been analyzed to reconstruct the marine $^{187}Os/^{188}Os$ record. However, records constructed from these materials are of low temporal resolution due to slow accumulation rates; furthermore, age control is poor due to the absence of microfossils. Thus, we consider metalliferous sediments to be superior to Mn crusts and pelagic clays as recorders of past changes in the $^{187}Os/^{188}Os$ composition of seawater, and have chosen to limit the current study to these deposits. Metalliferous sediments from the South Pacific Ocean (Sites 597 and 598, [27]) and South Atlantic Ocean (Site 521, [28])

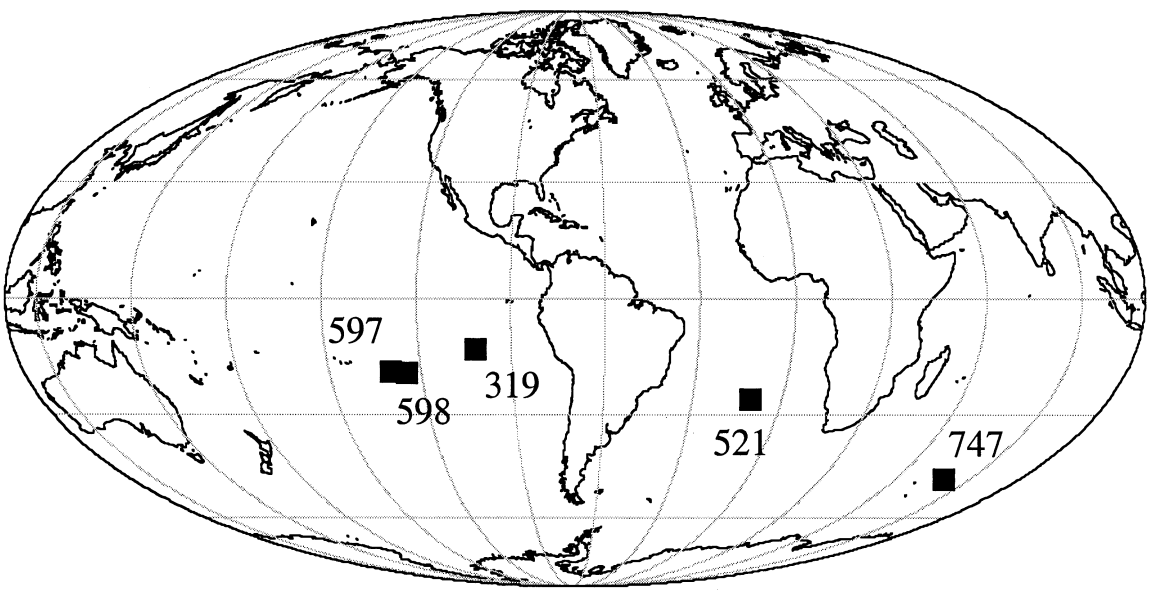

Fig. 2. Map showing locations of DSDP Sites 319, 521, 597, 598, and 747.

were investigated (Fig. 2). Site 598 is among those previously investigated [11] at very low temporal resolution (fewer than one analysis/10^6 yr) and was resampled to construct a higher resolution record through the Middle Miocene. Osmium isotopic analyses were made at fourteen levels, approximately every 2 m (three analyses/10^6 yr).

3. Methods

The majority of samples analyzed in this study were subjected to a two-step leaching procedure similar to that described by Peucker-Ehrenbrink et al. [18]. Calcium carbonate was first dissolved with acetic acid, then Fe- and Mn-oxides were dissolved in a sulfuric acid–hydrogen peroxide solution. The acetic acid leach was archived and Os was separated from the sulfuric acid–hydrogen peroxide solution. The peroxide leaching method was originally developed to selectively release seawater-derived Os from the large background of terrigenous and cosmic Os in pelagic clays [12]. To establish the reproducibility of this procedure, we made duplicate analyses of leaches from splits of five different sample powders. In addition to the leaching procedure, four samples from Site 598 were subjected to bulk analysis by NiS fire assay [29]. Splits of the sample powders chosen for bulk analyses were also subjected to the leaching procedure, affording a direct comparison of bulk and leach data. In both procedures, samples were spiked with isotopically enriched ^{190}Os so that Os concentrations could be determined by isotope dilution. In this study, the main advantage of the leaching procedure relative to bulk analysis was the very low procedural blank. Several grams of sample powder can be leached with a total procedural blank of approximately 0.2 pg Os. (For bulk analyses, the blank corrections involve concentrations of approximately 3.2 pg Os/g sample and ^{187}Os/^{188}Os ratio of 0.37.)

Following either the sediment leaching procedure or the fire assay procedure, Os was separated by distillation of OsO_4 into HBr. The distilled Os was further purified using a single-bead ion exchange method [30]. Osmium isotopes were measured as OsO_3^- by negative-ion thermal ionization mass spectrometry [31]. Ratios of measured intensities were corrected for instrumental mass fractionation and oxides in order to obtain atom ratios. Measured oxide ratios typically have standard errors, based on in-run counting statistics, between 0.2 and 0.3% (2σ). Because most of the previous work on Os isotopic variations in seawater has reported variations in the abundance of ^{187}Os in terms of ^{187}Os/^{186}Os

ratios, figures and tables present both 186-normalized and 188-normalized data (Table 1). In the text, Os isotopic variations are discussed in terms of 188-normalized data. Rhenium was monitored at the 249 and, intermittently, 233 mass peaks. The analysis of sample 5-1L from DSDP 598 appears to be the only one in which a Re interference correction is potentially significant. The corrected ratio (Table 1) is 0.5% less than the uncorrected ratio.

For Site 598, O and C isotopes were measured from 34 samples spaced approximately 1/m (8/Myr). Planktonic (*Dendoglobigerina altispira*, *Sphaeroidinellopsis seminulina*) and benthic species (*Globocassidulina subglobossa*, *Oridorsalis* spp., *Planulina wuellerstorfi*) were picked from the coarse (>250 μm) fraction. The benthic foraminiferal stable isotope record (Table 2) is based primarily on specimens of *Oridorsalis* spp., which were common in most samples. In samples without *Oridorsalis* spp., other species were analyzed and the species correction values reported in [32] were applied. For each sample, two to three foraminifera were dissolved in phosphoric acid at 90ºC and analyzed at the University of Maine on a VG/Fisons Prism Series II mass

Table 1
Depth, age, OS concentrations, and $^{187}Os/^{186}Os$, $^{187}Os/^{188}Os$ ratios (2σ in-run uncertainties are given for both ratios) for DSDP metalliferous sediments from the Pacific and Atlantic oceans

DSDP identifier leg–site, core-section, cm	Type [a]	Depth (mbsf)	Age (Ma)	$^{187}Os/^{186}Os$	$^{187}Os/^{188}Os$	Os (ng/g)
92–598, 3-2, 15–20	Br	17.45	10.96	6.592 ± 0.008	0.7910 ± 0.0009	0.086
	L			6.594 ± 0.011	0.7913 ± 0.0013	0.012
	Ld			6.502 ± 0.010	0.7802 ± 0.0012	0.020
92–598, 3-5, 104–108	L	22.84	12.03	6.679 ± 0.010	0.8015 ± 0.0012	0.022
92–598, 3-6, 24–28	B	23.54	12.17	6.623 ± 0.011	0.7948 ± 0.0013	0.061
	L			6.466 ± 0.034	0.7759 ± 0.0040	0.020
92–598, 4-1, 14–21	L	25.54	12.56	6.505 ± 0.008	0.7806 ± 0.0010	0.043
92–598, 4-2, 11–15	Bd	27.01	12.85	6.368 ± 0.017	0.7642 ± 0.0021	0.082
	L			6.363 ± 0.011	0.7636 ± 0.0013	0.020
92–598, 4-3, 86–90	L	29.26	13.30	6.442 ± 0.021	0.7730 ± 0.0026	0.045
92–598, 4-4, 14–19	Br	30.04	13.46	6.400 ± 0.011	0.7680 ± 0.0013	0.084
92–598, 4-4, 113–116	L	31.03	13.65	6.313 ± 0.013	0.7576 ± 0.0015	0.041
92–598, 4-6, 11–14	B	33.01	14.05	6.379 ± 0.024	0.7655 ± 0.0028	0.130
	L			6.439 ± 0.023	0.7727 ± 0.0028	0.037
	Ld			6.421 ± 0.017	0.7705 ± 0.0020	0.022
92–598, 5-1, 40–44	L	35.40	14.52	6.460 ± 0.009	0.7752 ± 0.0011	0.046
92–598, 5-2, 102–105	L	37.52	14.94	6.240 ± 0.010	0.7488 ± 0.0012	0.034
	Ld			6.212 ± 0.017	0.7454 ± 0.0021	0.052
92–598, 5-4, 10–14	L	39.60	15.27	6.254 ± 0.016	0.7505 ± 0.0019	0.058
92–598, 5-4, 20–25	Br	39.70	15.28	6.188 ± 0.006	0.7426 ± 0.0007	0.164
	L			6.320 ± 0.006	0.7584 ± 0.0008	0.069
92–598, 5-5, 58–62	L	41.58	15.55	6.379 ± 0.010	0.7655 ± 0.0011	0.047
	Ld			6.409 ± 0.014	0.7691 ± 0.0017	0.060
92–598, 5-6, 14–17	B	42.64	15.70	6.391 ± 0.006	0.7669 ± 0.0008	0.144
	L			6.357 ± 0.011	0.7628 ± 0.0014	0.034
	Ld			6.395 ± 0.013	0.7674 ± 0.0016	0.065
92–597, 3-1, 85–90	Br	15.10	18.90	6.122 ± 0.013	0.7346 ± 0.0015	0.038
	L			6.179 ± 0.015	0.7415 ± 0.0018	0.009
73–521, 13-3, 60–65	L	54.60	7.60	7.020 ± 0.011	0.8424 ± 0.0013	0.009
73–521, 16-1, 75–80	L	62.25	10.60	6.800 ± 0.014	0.8160 ± 0.0016	0.029
73–521, 17-3, 67–72	L	69.67	14.10	6.360 ± 0.030	0.7632 ± 0.0036	0.007
73–521, 18-3, 35–40	L	73.85	14.50	6.290 ± 0.018	0.7548 ± 0.0022	0.009
73–521, 19-2, 89–94	L	77.29	15.00	6.222 ± 0.011	0.7466 ± 0.0013	0.009
73–521, 20-2, 102–107	L	81.82	15.50	5.930 ± 0.031	0.7116 ± 0.0037	0.010

[a] B = bulk sample; L = peroxide leach; d = duplicate; r = from Ref. [11].

Table 2
Oxygen and carbon isotope data for benthic foraminifera, DSDP Site 598

Core-section, cm	Depth (mbsf)	Age (Ma)	Species [a]	$\delta^{13}C$	$\delta^{18}O$
3-5, 104–108	22.80	12.02	CW	1.14	2.55
			OR	−0.36	2.58
3-6, 31–36	23.61	12.18	OR	−0.02	2.64
3-6, 82–86	24.12	12.28	OR	0.11	3.01
4-1, 14–21	25.54	12.56	CW	1.27	2.63
4-1, 71–76	26.11	12.68	OR	0.47	2.65
4-1, 130–134	26.70	12.79	CW	1.41	2.09
			OR	0.49	2.78
4-2, 41–46	27.31	12.91	SUB	1.01	2.60
4-3, 19–23	28.59	13.17	OR	0.60	2.19
4-3, 86–90	29.26	13.30	SUB	1.55	3.09
4-3, 146–149	29.86	13.42	OR	0.36	2.33
4-4, 61–66	30.51	13.55	OR	0.65	2.55
4-4, 113–116	31.03	13.65	OR	0.88	2.57
4-5, 13–17	31.53	13.75	OR	0.73	2.61
4-5, 71–74	32.11	13.87	OR	0.47	2.27
4-6, 32–37	33.22	14.09	Csp	1.08	1.18
			OR	0.31	2.30
5-1, 40–44	35.40	14.52	OR	0.91	1.85
5-1, 91–95	35.91	14.62	OR	0.07	1.87
5-1, 141–146	36.41	14.72	SUB	1.14	1.57
5-2, 51–56	37.01	14.84	OR	−0.08	1.78
5-2, 102–105	37.52	14.94	OR	0.84	1.95
			SUB	1.11	1.61
5-3, 0–4	38.00	15.04	OR	0.52	1.72
5-3, 52–55	38.52	15.12	SUB	0.87	1.90
5-3, 107–110	39.07	15.19	OR	0.65	1.74
5-4, 10–14	39.60	15.27	OR	−0.03	1.48
5-4, 62–65	40.12	15.34	OR	0.36	1.88
5-4, 110–113	40.60	15.41	OR	0.49	1.58
5-5, 6–9	41.06	15.48	OR	0.57	1.76
5-5, 58–62	41.58	15.55	SUB	1.18	1.90
			SUB	1.18	1.88
5-5, 93–96	41.93	15.60	OR	0.44	1.78
5-5, 143–146	42.43	15.67	OR	0.45	1.67
5-cc, 0–4	43.26	15.79	OR	0.62	2.02
			SUB	1.15	1.86

[a] Cb = *Cibicidoides* spp.; CW = *Planulina wuellerstorfi*; OR = *Oridorsalis* spp.; SUB = *Globocassidulina subglobossa*.

spectrometer. Samples of bulk carbonate were also analyzed (Table 3).

4. Stratigraphy

The age model for Site 521 is tightly constrained by magnetostratigraphy [33] and calcareous nannofossil and planktonic foraminiferal biostratigraphy [34,35]. In order to compare the high resolution Os isotopic record from Site 598 with records from other sites, we supplemented published calcareous nannofossil [36] and planktonic foraminiferal biostratigraphy [37] with higher resolution planktonic foraminiferal biostratigraphy and benthic foraminiferal stable isotope stratigraphy. All ages are reported according to the time scale in [38].

The shipboard planktonic foraminiferal biostratigraphy for Site 598 was limited to core catcher samples [37], yielding large uncertainties (±4.8 m) in the placement of four zonal boundaries. We refined this stratigraphy with samples taken every 0.75 m or

Table 3
Oxygen and carbon isotope data from bulk carbonate, DSDP Site 598

Core-section, cm	Depth (mbsf)	Age (Ma)	$\delta^{13}C$	$\delta^{18}O$
3-5, 104–108	22.84	12.03	1.82	1.40
3-6, 31–36	23.61	12.18	2.28	1.58
3-6, 82–86	24.12	12.28	2.23	1.50
4-1, 14–21	25.54	12.56	2.29	1.53
4-1, 71–76	26.11	12.68	2.02	1.32
4-1, 130–134	26.70	12.79	2.17	1.47
4-2, 106–110	27.96	13.04	2.29	1.22
4-3, 86–90	29.26	13.30	2.29	1.12
4-3, 146–149	29.86	13.42	2.55	0.97
4-4, 61–66	30.51	13.55	2.34	1.17
4-4, 113–116	31.03	13.65	2.51	1.40
4-5, 13–17	31.53	13.75	2.59	1.78
4-5, 71–74	32.11	13.87	2.40	1.40
4-5, 115–119	32.55	13.95	2.37	1.49
4-6, 32–37	33.22	14.09	2.43	1.48
5-1, 40–44	35.40	14.52	2.42	0.99
5-1, 91–95	35.91	14.62	2.24	1.08
			2.19	0.93
5-1, 141–146	36.41	14.72	2.36	1.11
5-2, 51–56	37.01	14.84	2.42	1.43
5-2, 102–105	37.52	14.94	2.47	1.09
			2.46	1.11
5-3, 0–4	38.00	15.04	2.63	1.06
5-4, 10–14	39.60	15.27	2.22	0.52
5-4, 62–65	40.12	15.34	2.39	1.11
5-4, 110–113	40.60	15.41	2.06	0.93
5-5, 6–9	41.06	15.48	2.27	1.25
5-5, 58–62	41.58	15.55	2.17	0.49
5-5, 93–96	41.93	15.60	2.29	1.09
5-5, 143–146	42.43	15.67	2.33	0.90
5-6, 30–33	42.80	15.73	2.32	0.90
5-cc, 0–4	44.00	15.90	2.51	0.62

closer, recognizing six zones (N8–N14) based on the criteria of Blow [39] (Table 4). The uppermost sample (Sample 92-598-3-5, 104–108 cm) contains the only occurrence of *Globigerina nepenthes*, placing it just above the Zone N14/N13 boundary (11.8 Ma). The first appearance of *Orbulina suturalis* (Zone N8/N9 boundary, 15.1 Ma) occurs between Samples 92-598-5-3, 0–4 cm and 92-598-5-3, 52–55 cm at a level of 38.26 mbsf. Specimens of this species and *Orbulina universa* are common above this level. Our lowermost sample (Sample 92-598-5 cc) contains *Globigerina sicanus*, indicating that this level is still within Zone N8 and is younger than 16.4 Ma. Also, Romine [37] found *G. sicanus* just below this level in Sample 92-598-6 cc. Planktonic foraminifera show evidence of dissolution in most of the interval studied, making the placement of the zonal boundaries N10/N9 to N13/N12 less certain. We suspect that the first appearance of *Globorotalia peripheroacuta* (N10/N9, 14.8 Ma) at Site 598 is not a true datum as this species was only sporadically found. Furthermore, only one sample from Site 598 contains specimens of the *Globorotalia fohsella* group, whose first and last appearances are important markers for the tops of Zones N10 to N12. As a result, we used only the three planktonic foraminiferal datums considered to be reliable in the age model (Table 4).

The benthic foraminiferal $\delta^{18}O$ and $\delta^{13}C$ records further constrain the age model for Site 598, according to the oxygen-isotopic scheme of [40,41] and carbon-isotopic scheme of Woodruff and Savin [42]. The Mi3 (13.6 Ma) and Mi4 (12.8 Ma) $\delta^{18}O$ maxima were identified at levels 31.50 and 25.54 mbsf, respectively (Table 4). The Middle Miocene $\delta^{18}O$ increase preceding the Mi3 maximum at Site 598 begins at 36.41 mbsf. In records with reliable magnetostratigraphy, this increase begins near the top of magneto-chron C5Bn which has an age estimate of 14.8 Ma [41]. The $\delta^{18}O$ record does not show a maximum correlative with the Mi2 maximum suggesting that the lowestmost sample is younger than 16.0 Ma. The $\delta^{13}C$ record from Site 598 shows a prominent maximum at 31.50 mbsf interpreted as CM6, having an age estimate of 13.8 Ma [42].

A simple linear age model (age $= 0.1986 \times$ depth $+ 7.4902$) was applied to the calcareous nannofossil, planktonic foraminiferal, and stable isotopic datums in the top part of the Site 598 core (above 38.26 m) to provide age estimates for each sample level. Higher sedimentation rates, which are expected due to proximity to hydrothermal sources and shallower paleodepths, are indicated by the absence of Mi2 in the sampled interval. A second regression ($0.1425 \times$ depth $+ 9.6267$) was applied to the datums below 38.26 m.

5. Results and discussion

5.1. Comparison of bulk and leaching techniques

Duplicate leaches of five sediment samples yielded an average difference of 0.6% (0.005

Table 4
List of biostratigraphic and stable isotopic datum levels used to construct age model for Site 598

Datum	Type	Age (Ma)	Depth (mbsf)	Reference
1 CN6/CN7	nannofossil	10.7	16.10	[38]
2 CN5/CN6	nannofossil	10.9	16.85	[38]
3 FAD[a] *Globigerina nepenthes*	foraminifera	11.8	23.23	this study
4 Mi4	$\delta^{18}O$	12.8	25.54	this study
5 CN4/CN5	nannofossil	13.6	29.75	[38]
6 Mi3	$\delta^{18}O$	13.6	31.50	this study
7 CM 6	$\delta^{13}C$	13.6	31.50	this study
8 Base $\delta^{18}O$ increase	$\delta^{18}O$	14.8	36.41	this study
9 FAD *Orbulina suturalis*	foraminifera	15.1	37.80	this study
10 Mi2[b]	$\delta^{18}O$	<16.0	43.26	this study
11 FAD *Globigerina sicanus*	foraminifera	16.4	44.75	[39]

[a] FAD, first appearance datum.
[b] Mi2 is below this level.

$^{187}Os/^{188}Os$ units). The difference between duplicate leaches ranges from 0.3 to 1.4% (Table 1). These duplicate analyses establish an empirical limit at which true differences in isotopic composition can be resolved. Seven samples were analyzed using both the selective leaching procedure and a procedure involving total sediment digestion by fire assay. Corresponding 'bulk–leach' pairs differ by an average of 1% (0.008 $^{187}Os/^{188}Os$ units), an amount slightly larger than the average difference between duplicate leach analyses. The difference between bulk–leach pairs ranges from 0.1 to 2.4% (0.001 to 0.019 $^{187}Os/^{188}Os$ units).

In essence, the $^{187}Os/^{188}Os$ ratios measured from bulk and leach analyses of the Site 598 samples do not differ systematically. A similar result was obtained from other metalliferous sediment samples [18]. The good agreement between bulk and leach analyses of the Os isotopic composition of metalliferous sediments implies that the Os in these sediments is almost entirely derived from a seawater source.

5.2. Geographic variations

The Atlantic (Site 521) and Pacific (Site 598) metalliferous carbonate records reveal no systematic differences in $^{187}Os/^{188}Os$ ratios through the Middle Miocene (Fig. 1). They are indistinguishable at the level of our external reproducibility ($\pm$0.005 $^{187}Os/^{188}Os$ units), providing empirical evidence that the oceanic residence time of Os is long enough for Os to have become well-mixed in the Miocene oceans. Thus, our measurements reflect global variations in the $^{187}Os/^{188}Os$ ratio of seawater.

Excellent agreement between Pacific and Atlantic data also supports our contention that metalliferous sediments are superior to pelagic clays as recorders of past variations in the Os isotopic composition of seawater. All in all, there is much less scatter in the $^{187}Os/^{188}Os$ ratios from metalliferous carbonates than from combined pelagic clays and metalliferous carbonates [18]. In Pacific sediments, the pelagic clay data show significantly more scatter between cores [18] than do the two metalliferous sediment records from different ocean basins.

The Atlantic Ocean may have developed slightly higher $^{187}Os/^{188}Os$ ratios than the Pacific Ocean from the Middle Miocene to the present. Although sensitive to errors in temporal correlation, our two uppermost Atlantic samples, of Late Miocene age, are higher by 0.015 $^{187}Os/^{188}Os$ units than the mean Pacific values. Studies of modern Mn crusts indicate that $^{187}Os/^{188}Os$ ratios are systematically higher, by 0.022 units, in the North Atlantic than in the Pacific and Indian oceans [26]. If our records are representative of the Miocene ocean and if the Mn crust data are truly representative of the Os isotopic variations in the modern ocean, then these data collectively suggest that Os in the Middle Miocene ocean was more nearly homogeneous than in the modern ocean. Changes in the pattern of deep water formation provide a potential explanation allowing us to reconcile this apparent discrepancy. During the Middle

Miocene, there may not have been an equivalent to North Atlantic Deep Water (NADW); rather, deep waters of both the Pacific and Atlantic oceans show $\delta^{13}C$ gradients suggesting a single southern (Antarctic) source [41,43].

5.3. Long-term temporal variations

The trend of increasing $^{187}Os/^{188}Os$ ratios from the Middle Miocene to the present noted by Ravizza [11] has been confirmed. The inflection between this increasing trend and almost constant ratios through the Early Miocene and Late Oligocene occurs no later than 16 Ma (Fig. 3b). The estimated $^{187}Os/^{188}Os$ composition of average continental crust is 1.2–1.3 [44]; riverine $^{187}Os/^{188}Os$ ratios are generally higher [13,45]. Increasing marine $^{187}Os/^{188}Os$ ratios after 16 Ma were almost certainly caused by an increasing contribution of radiogenic Os from continental sources, either sialic materials or old organic matter. Specifically, shales host abundant organic matter, which scavenges Os and, to a greater extent, Re; consequently, their Re/Os ratios are high [46,47], and calculations indicate that these sources attain elevated $^{187}Os/^{188}Os$ ratios within several million years.

5.3.1. Os–C comparisons

Bulk carbonate $\delta^{13}C$ values generally decrease through the Neogene from relatively high values in the Middle Miocene [48,49]. In DSDP 598, the shift toward lower bulk carbonate $\delta^{13}C$ values began around 13.6 Ma (Fig. 3c). This decrease in $\delta^{13}C$ values apparently lags the increase in $^{187}Os/^{188}Os$ ratios by more than 2 Myr.

Decreases in marine bulk carbonate $\delta^{13}C$ values can result from decreased organic C burial [50] or decreased fractionation [51]. Alternatively, they can result from increased weathering of organic matter with low $\delta^{13}C$ values [7,11]. Ravizza specifically suggested that the Neogene increase in $^{187}Os/^{188}Os$ ratios and decrease in bulk carbonate $\delta^{13}C$ values are both a consequence of increased weathering of organic matter [11]. The mean age of the weathered organic matter is critically important to models linking the marine $\delta^{13}C$ and $^{187}Os/^{188}Os$ records in this manner [52] (i.e. the organic matter must be sufficiently old to have attained elevated $^{187}Os/^{188}Os$ ratios).

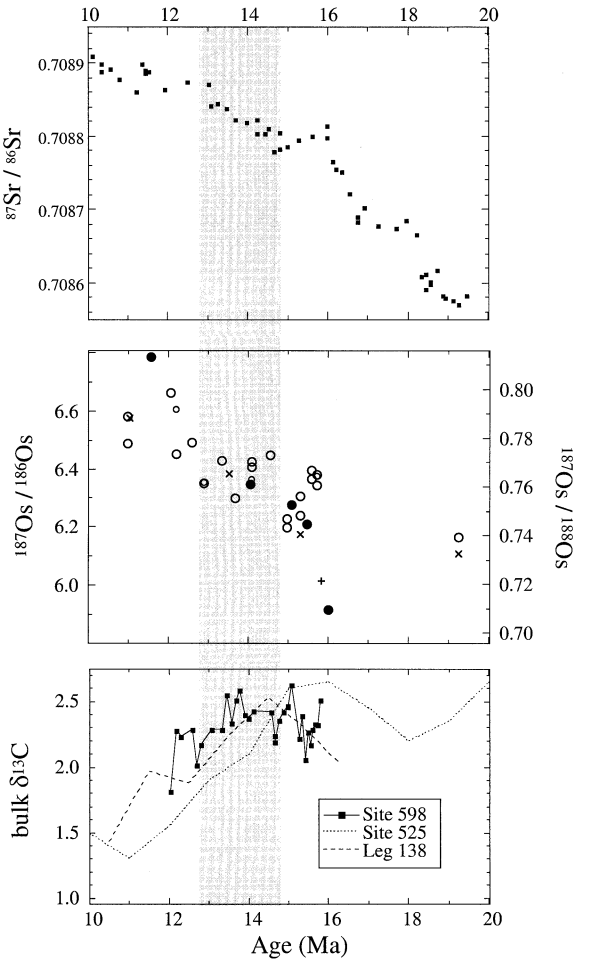

Fig. 3. (a) Marine $^{87}Sr/^{86}Sr$ record from DSDP 747A for the period 20–10 Ma [20]. Note the prominent decrease in rate of increase at 16 Ma. (b) $^{187}Os/^{188}Os$ record for the period 20–10 Ma, showing increase beginning no later than 16 Ma. Symbols are the same as in Fig. 1. (c) $\delta^{13}C$ of marine bulk carbonate. Note that the Neogene decrease began during the Middle Miocene around 13.6 Ma. Also shown are averaged $\delta^{13}C$ values of bulk carbonate from Site 525 [53] and Leg 138 [48]. The vertical shaded bar shows the interval, from 14.8 to 12.8 Ma, of the Middle Miocene positive shift in $\delta^{18}O$ values (Fig. 1a).

Increased weathering of organic matter implies an almost exact temporal correspondence between increases in the resulting C and Os fluxes, but not necessarily an exact temporal correspondence between decreasing $\delta^{13}C$ values and increasing $^{187}Os/^{188}Os$ ratios.

Accelerated organic C weathering does not neces-

sarily imply diminished organic C burial. Rather, the inferred exhumation that permits organic C weathering also implies conditions favorable for enhanced burial and preservation of organic C, specifically high sedimentation rates of fine-grained materials [53] and nutrient-loading of both terrestrial and marine ecosystems [54]. If C and Os fluxes were coupled during Miocene organic C weathering, then the more than 2 Myr lag of the bulk carbonate $\delta^{13}C$ decrease relative to the $^{187}Os/^{188}Os$ increase observed in DSDP 598 implies excess organic C burial between 16 and 13.6 Ma. In this regard, the occurrence of organic C-rich deposits in the Monterey Formation deposited during this interval [4] provides support for the geochemical linkage proposed by Ravizza [11]. Accelerated organic C weathering also does not necessarily imply increasing atmospheric pCO_2 if the organic C burial and silicate weathering sinks keep pace.

5.3.2. Os–Sr comparisons

The rate of increase of marine $^{87}Sr/^{86}Sr$ ratios decreased at 16 Ma (Fig. 3a), according to the inflection in the Site 747A record near the base of magneto-chron C5B [17]. This plateau in an otherwise increasing trend lasted 3–4 Myr. Site 747A is tightly constrained by magnetostratigraphy; less well-constrained $^{87}Sr/^{86}Sr$ records show the plateau in $^{87}Sr/^{86}Sr$ ratios beginning sometime between 16 and 15.4 Ma.

The $^{87}Sr/^{86}Sr$ ratios of sources affecting seawater range from 0.7035 for hydrothermal discharges from basalts through around 0.708 for dissolution of pelagic carbonates to over 0.71 for rivers [10,55]. Rivers draining sialic crust typically contain highly radiogenic Sr at very low concentrations. Significant contributions of ^{87}Sr are expected only from Himalayan-type crust in which ^{87}Sr is thought to have been metamorphically partitioned from relatively insoluble Rb-rich minerals (e.g. K-feldspars) into more soluble Ca-bearing phases such as plagioclase, biotite, and calcite [56–59]. The steep Early Miocene increase in $^{87}Sr/^{86}Sr$ ratios has been correlated with development of the Himalayan Main Central Thrust–South Tibetan detachment system [6,54,60]; recent findings [59] trace high riverine $^{87}Sr/^{86}Sr$ ratios to radiogenic calcites (the weathering of which does not affect long-term atmospheric pCO_2, [3]). Possible mechanisms for the Middle Miocene $^{87}Sr/^{86}Sr$ plateau include an increase in nonradiogenic Sr from basalt weathering [21], an increase in intermediate Sr from carbonate weathering or submarine dissolution [8], and a decrease in radiogenic Sr from the Himalayas [6].

The Late Oligocene through Middle Miocene $^{187}Os/^{188}Os$ and $^{87}Sr/^{86}Sr$ records are conspicuously decoupled. Whereas $^{87}Sr/^{86}Sr$ ratios became nearly constant at 16 Ma, $^{187}Os/^{188}Os$ ratios began to increase at this time [11]. If both $^{87}Sr/^{86}Sr$ and $^{187}Os/^{188}Os$ ratios were responding primarily to the same radiogenic source, as was first suggested [12], then they should have varied almost in tandem (with only minor lag in the Sr signal, on the order of 1 Myr, due to the longer response time of Sr). The decoupling around 16 Ma therefore suggests that weathering of sediments, rather than of ancient crust, dominates the Early and Middle Miocene Os signal.

5.3.3. Specific geologic mechanisms for isotopic variations

A limited number of Miocene events involve significant exhumation of rock assemblages capable of simultaneously supplying the ocean with radiogenic Os and nonradiogenic (or soluble intermediate) Sr and thus causing the inflections in both marine records at 16 Ma. These include the emergence of continental margins in the Australia–Indonesian region and the first glaciation of sediment-veneered continental interiors in the Northern Hemisphere. The Os isotopic data cannot be readily explained by scenarios involving either the Columbia River flood basalt eruptions around 16 Ma [6] or the initiation of the Main Central Thrust–South Tibetan detachment system between 21 and 17 Ma [54].

The most plausible tectonic mechanism for Middle Miocene decoupling of the $^{187}Os/^{188}Os$ and $^{87}Sr/^{86}Sr$ records is the collision between New Guinea and Australia [21] and general emergence of Indonesia. A prominent Middle Miocene unconformity, sculpted into the northern New Guinea arc terrane, and orogenic sediments in the Australian foreland lend support to this scenario [61]. Specifically, the foreland basin, derived primarily from the Australian margin, developed between the Early Miocene and late Middle Miocene [61]. The uplifted arc material is likely to be a major source of non-

radiogenic Sr and potential cause of the $^{87}Sr/^{86}Sr$ plateau. The Australian continental margin, in addition to being a major source of intermediate Sr in carbonates, is likely to be a major source of radiogenic Os, both in sialic crust and in the rifted margin sediments (mean age approximately 50 Ma). The magnitude of exhumation should have been on the order of exhumation experienced in the early Himalayan collision [7].

The emergence of New Guinea and other parts of Indonesia offers a mechanism for both the Middle Miocene cooling event and the preceding thermal optimum. A reduced greenhouse effect brought on by the increased availability in the northern volcanic arc terrane of highly soluble Ca and Mg silicates would have been preceded by an increased greenhouse effect associated with weathering of the sedimentary arc [7]. The lag between the warming and cooling events corresponds closely with the estimated time it would take for the Australian plate to underthrust the trench–arc system, which is 2.5 Myr based on an average separation of 200 km between sedimentary and volcanic arcs and a convergence rate of 8 cm/yr.

An alternative explanation for both the $^{187}Os/^{188}Os$ and $^{87}Sr/^{86}Sr$ records is Northern Hemisphere glaciation, which began earlier (Middle Miocene) than previously thought [62]. The first continental glaciers in the Northern Hemisphere should have delivered radiogenic Os, from old sediments and crust, and intermediate Sr, from carbonates, to the ocean. Pulses of ice-rafted debris have recently been recognized in the North Atlantic Ocean at times corresponding with the Mi3 and Mi4 $\delta^{18}O$ maxima [62]. Especially the earliest glaciations of the northern continents would have eroded primarily the cratonic sedimentary cover, which we speculate meets the criteria for a ^{187}Os-enriched/^{87}Sr-depleted source.

An appealing feature of the Northern Hemisphere glaciation scenario is its ability to account for the possible Os isotopic heterogeneity suggested by the slightly contrasting post-Middle Miocene records from the Atlantic and Pacific basins. If NADW is the main carrier of radiogenic Os into the Atlantic, then the more radiogenic Atlantic Os isotopic ratios point to glacial erosion of sediment-covered cratons as a source of radiogenic Os that contributed to the Neogene increase in marine $^{187}Os/^{188}Os$ ratios.

An issue with Northern Hemisphere glaciation as a cause of the Neogene Os isotopic increase is the small size of the first ice sheets in the Northern Hemisphere, as indicated by the limited extent of ice-rafted debris during the Middle Miocene [62]. Also, the Atlantic Ocean did not attain (possible) elevated $^{187}Os/^{188}Os$ ratios until after the Middle Miocene, well after the beginning of the long-term increase in $^{187}Os/^{188}Os$ ratios (16 Ma).

5.4. High resolution 598 record

For the first time, both $^{187}Os/^{188}Os$ analyses and stable isotopic analyses have been made from the same metalliferous carbonate samples. This approach, by avoiding the uncertainties associated with correlating between cores, permits ready comparison between the $^{187}Os/^{188}Os$ and stable isotopic data. We restrict the interpretation of fine structure to leach analyses from DSDP 598 because of the relatively large uncertainties stemming from blank corrections in the fire assay step of bulk sample analyses and because of age uncertainties associated with correlating between cores. Post-burial decay of Re produces radiogenic Os; however, metalliferous carbonates are unlikely to have significant Re [25,63]. Although we have not made corrections for in situ production of ^{187}Os, an upper limit is likely to be around 0.3% based on a sample from DSDP 597 [18].

The high resolution data from Site 598 suggest a weak oscillatory structure in the $^{187}Os/^{188}Os$ record with amplitudes on the order of 0.01 to 0.02 and frequencies of 1/Myr or higher (Fig. 4b). The amplitudes of these oscillations are two to four times as large as the mean difference (0.005 $^{187}Os/^{188}Os$) between duplicate leach analyses (the envelope on Fig. 4b is defined by this mean difference). Relatively high $^{187}Os/^{188}Os$ ratios (0.76 to 0.77) in the oldest samples imply an increasing trend leading to a maximum around 15.5 Ma. A well-defined decrease from 0.77 to 0.75 occurs in the most densely sampled interval between 15.5 and 14.9 Ma. At the current density of sampling, the record appears to have maxima around 15.5 Ma, 14.5 Ma, and possibly 13.3 Ma. Minima occur prior to 15.5 Ma, around 15 Ma, and possibly near 13.7 Ma and 12.8 Ma. In addition to the need for higher resolution sampling at Site 598 to better define the suggested oscilla-

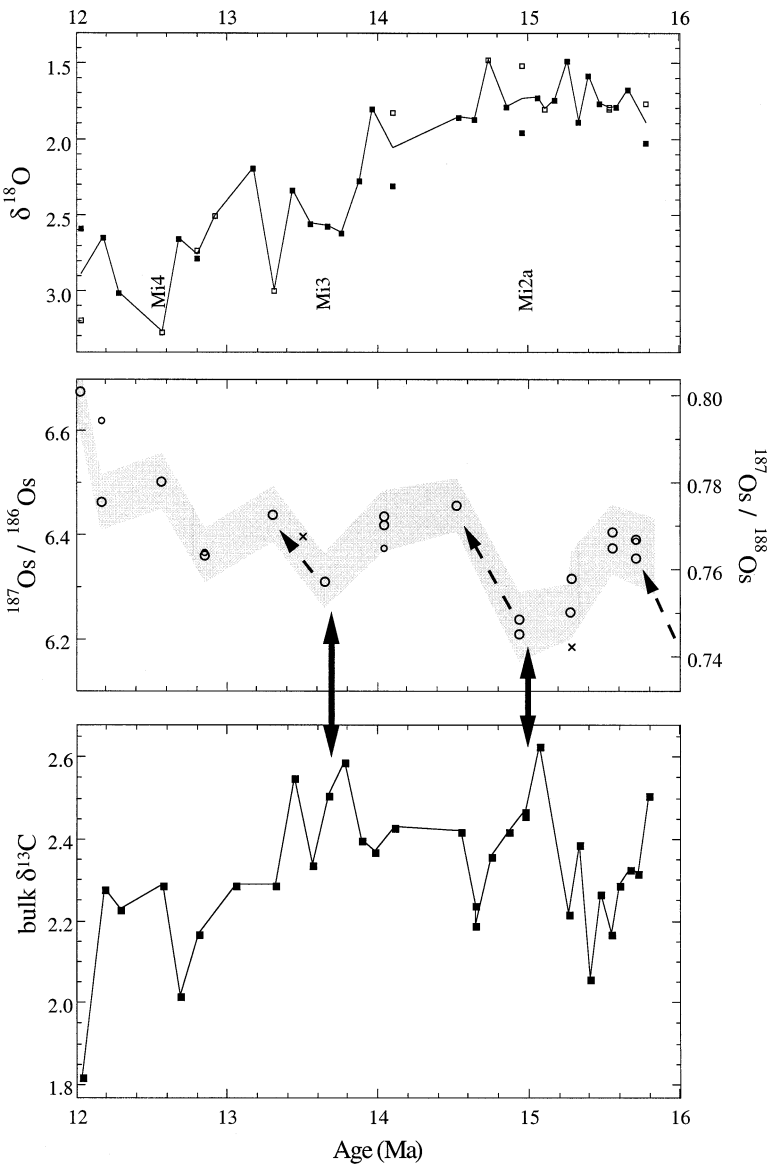

Fig. 4. (a) Benthic foraminiferal $\delta^{18}O$ values from DSDP Site 598, measured on *Oridorsalis* spp. (solid squares) and *G. subglobossa* and *P. wuellerstorfi* (open squares). The Mi2a (15 Ma), Mi3 (13.6 Ma), and Mi4 (12.8 Ma) maxima are indicated. (b) High resolution $^{187}Os/^{188}Os$ analyses from Site 598. Large circles are leached samples and small circles are bulk analyses. The envelope is defined by the mean difference between duplicate leaches (0.005 $^{187}Os/^{188}Os$ units). Crosses are from [14]. Dashed arrows indicate increases following Mi maxima. Solid arrows show inverse correlation with bulk carbonate $\delta^{13}C$ values. (c) Bulk carbonate $\delta^{13}C$ values from Site 598. The possible inverse correlation of Os with O and C isotopes suggests a common glacioeustatic control.

tions, it must be emphasized that additional analyses from other cores are required to determine whether the DSDP 598 Os signal is representative of whole-ocean variations in the Os isotopic composition of seawater.

With the caveat that fine structure in the $^{187}Os/^{188}Os$ record has not been proven to represent a global signal, our data appear to vary in an inverse manner with respect to benthic foraminiferal $\delta^{18}O$ values (Fig. 4a) in the sense suggested by [64]

for Pleistocene glacial–interglacial cycles (but on a time scale two orders of magnitude larger). The inferred pre-15.5 Ma $^{187}Os/^{188}Os$ increase follows the Mi2 (glacial) maximum (16 Ma). The second $^{187}Os/^{188}Os$ increase follows the Mi2a maximum at 15 Ma. The third possible $^{187}Os/^{188}Os$ increase follows the Mi3 maximum. If these correlations persist in higher resolution records, the mechanism for the $^{187}Os/^{188}Os$ increases probably involves the weathering of exposed glacial drift and continental shields during relatively humid deglaciations [13]. The physically ground, highly radiogenic continental materials would be ripe for chemical weathering. Pleistocene glacial terminations are characterized by warm and wet climates, optimal for chemical weathering, but the nature of climate following the Mi glacial maxima is not known in any detail.

The $^{187}Os/^{188}Os$ data may also vary in an inverse manner with respect to the bulk carbonate $\delta^{13}C$ record (Fig. 4c). Our bulk carbonate data show the same general features displayed by higher resolution bulk carbonate records from the Pacific [48] and Atlantic oceans [49]. All three of these records show strong maxima at 15 Ma and between 14 and 13.6 Ma followed by generally decreasing values. Minima in the $^{187}Os/^{188}Os$ record at 15 Ma and near 13.7 Ma match the two strong $\delta^{13}C$ maxima; the subsequent general increase in $^{187}Os/^{188}Os$ ratios corresponds with the general decrease in the bulk carbonate $\delta^{13}C$ values. The same mechanism [64] proposed for the inverse correlation between $^{187}Os/^{188}Os$ and benthic foraminiferal $\delta^{18}O$ may apply for $^{187}Os/^{188}Os$ and bulk carbonate $\delta^{13}C$. During deglaciations, old organic C is weathered, releasing C with low $\delta^{13}C$ values and radiogenic Os.

6. Conclusions

Combined Atlantic and Pacific samples demonstrate that seawater $^{187}Os/^{188}Os$ ratios were homogeneous in the Atlantic and Pacific oceans during the Middle Miocene, when production of Northern Component Water and Tethyan outflow water were curtailed [41]. The small Os isotopic contrast observed between the North Atlantic and the Pacific and Indian oceans in recent Mn crusts [26] suggests that the residence time of Os is poised very close to the mixing time of the oceans, and that North Atlantic Deep Water may be the vector presently delivering radiogenic Os to the global ocean.

No systematic differences were observed between bulk and leached sediment pairs, and high resolution data match the previously defined long-term trend —therefore contamination by cosmic dust is not a factor in rapidly deposited metalliferous carbonates that evidently contain mostly hydrogenous Os.

The large-scale decoupling of the $^{187}Os/^{188}Os$ and $^{87}Sr/^{86}Sr$ records in the Miocene can be explained by the emergence between 16 and 15 Ma of a source enriched in ^{187}Os and depleted in ^{87}Sr, in contrast to the previous mean source characterized by high $^{87}Sr/^{86}Sr$ and intermediate $^{187}Os/^{188}Os$ ratios. In the Early Miocene, the exhumation of Himalayan continental crust, with soluble ^{87}Sr-enriched phases, probably drove the rise in seawater $^{87}Sr/^{86}Sr$ ratios. In the Middle Miocene, we can suggest two scenarios. First, Northern Hemisphere ice sheets would have exhumed ^{187}Os-rich/^{87}Sr-rich sediments as they developed. Alternatively, during the Middle Miocene, both the Australian continental margin, a large source of ^{187}Os-enriched sediments and intermediate Sr, and the northern New Guinea arc terrane, a large source of ^{87}Sr-depleted volcanic rocks, were uplifted and eroded. In the second scenario, increased availability of soluble Ca and Mg silicates may have contributed to greenhouse cooling, although it remains to be shown that CO_2 levels decreased through the Middle Miocene $\delta^{18}O$ shift.

Fine-scale oscillations of $^{187}Os/^{188}Os$ in Pacific sediments have periods on the order of a million years and amplitudes of 0.01 to 0.02. These oscillations in sedimentary $^{187}Os/^{188}Os$ ratios are well resolved analytically but it remains to be established that they represent a global signal. With this caveat, some of these variations appear to correlate in an inverse fashion with the benthic foraminiferal $\delta^{18}O$ record, which is in the same sense as described by [64] for Pleistocene glacial cycles. Variations in bulk carbonate $\delta^{13}C$ through this period may also be linked to glacioeustatic processes. The global nature of the DSDP 598 record would best be tested by similar high resolution work on Atlantic core DSDP 521 to reproduce the same signal.

Acknowledgements

The first author was supported by a Harold T. Stearns Fellowship and also a University of Maine Association of Graduate Students grant. Samples for this program were provided by the International Ocean Drilling Program. Bernhard Peucker-Ehrenbrink and Jurek Blusztajn provided guidance with the $^{187}Os/^{188}Os$ analyses. The facilities and materials for the Os isotope analyses are supported by NSF grant 9301049. Detmar Schnitker helped with the identification of benthic foraminiferal taxa. Julie Friez picked the benthic foraminifera and Doug Introne performed the stable isotope analyses. Kevin Burton, John Chesley, and Franco Marcantonio provided constructive reviews of the original manuscript. ***[FA]***

References

[1] T.C. Chamberlin, An attempt to frame a working hypothesis of the cause of glacial periods on an atmospheric basis, J. Geol. 7 (1899) 545–584, 667–685, 751–787.

[2] H.D. Holland, The Chemistry of the Atmosphere and Oceans, Wiley, New York, 1978.

[3] R.A. Berner, A.C. Lasaga, R.M. Garrels, The carbonate–silicate geochemical cycle and its effect on atmospheric carbon dioxide over the past 100 million years, Am. J. Sci. 283 (1983) 641–683.

[4] E. Vincent, W.H. Berger, Carbon dioxide and polar cooling in the Miocene: the Monterey Hypothesis, in: E.T. Sunquist, W.S. Broecker (Eds.), The Carbon Cycle and Atmospheric CO_2: Natural Variations Archean to Present, Geophys. Monogr. Ser. 32 (1985) 455–468.

[5] M.E. Raymo, W.F. Ruddiman, P.N. Froelich, Influence of late Cenozoic mountain building on ocean geochemical cycles, Geology 16 (1988) 649–653.

[6] D.A. Hodell, F. Woodruff, Variations in the strontium isotopic ratio of seawater during the Miocene: Stratigraphic and geochemical implications, Paleoceanography 9 (1994) 405–426.

[7] R.A. Beck, D.W. Burbank, W.J. Sercombe, T.L. Olson, A.M. Khan, Organic carbon exhumation and global warming during the early Himalayan collision, Geology 23 (1995) 387–390.

[8] F.M. Richter, D.B. Rowley, D.J. DePaolo, Sr isotope evolution of seawater: The role of tectonics, Earth Planet. Sci. Lett. 109 (1992) 11–23.

[9] Y. Goddéris, L.M. François, The Cenozoic evolution of the strontium and carbon cycles: relative importance of continental erosion and mantle exchanges, Chem. Geol. 126 (1995) 169–190.

[10] M.R. Palmer, J.M. Edmond, The strontium isotope budget of the modern ocean, Earth Planet. Sci. Lett. 92 (1989) 11–26.

[11] G. Ravizza, Variations in the $^{187}Os/^{186}Os$ ratio of seawater over the past 28 million years as inferred from metalliferous carbonates, Earth Planet. Sci. Lett. 118 (1993) 335–348.

[12] W.J. Pegram, S. Krishnaswami, G. Ravizza, K.K. Turekian, The record of seawater $^{187}Os/^{186}Os$ variation through the Cenozoic, Earth Planet. Sci. Lett. 113 (1992) 569–576.

[13] B. Peucker-Ehrenbrink, G. Ravizza, Continental runoff of osmium into the Baltic Sea, Geology 24 (1996) 327–330.

[14] N.J. Shackleton, J.P. Kennett, Paleotemperature history of the Cenozoic and initiation of Antarctic glaciation: Oxygen and carbon isotopic analyses in DSDP Sites 277, 279, and 281, Init. Rep. DSDP 29 (1975) 743–755.

[15] K.G. Miller, R.G. Fairbanks, G.S. Mountain, Tertiary oxygen isotope synthesis, sea level history, and continental margin erosion, Paleoceanography 2 (1987) 1–19.

[16] D.J. DePaulo, K.L. Finger, High-resolution strontium-isotope stratigraphy and biostratigraphy of the Miocene Monterey Formation, central California, Geol. Soc. Am. Bull. 103 (1991) 112–124.

[17] J.S. Oslick, K.G. Miller, M.D. Feigenson, J.D. Wright, Oligocene–Miocene strontium isotopes: Stratigraphic revisions and correlations to an inferred glacioeustatic record, Paleoceanography 9 (1994) 427–444.

[18] B. Peucker-Ehrenbrink, G. Ravizza, A.W. Hofmann, The marine $^{187}Os/^{186}Os$ record of the past 80 million years, Earth Planet. Sci. Lett. 128 (1995) 591–599.

[19] F.M. Richter, K.K. Turekian, Simple models for the geochemical response of the ocean to climatic and tectonic forming, Earth Planet. Sci. Lett. 119 (1993) 121–131.

[20] M. Sharma, D.A. Papanastassiou, G.J. Wasserburg, The concentration and isotopic composition of osmium in the oceans, Geochim. Cosmochim. Acta 61 (1997) 3287–3299.

[21] D.N. Reusch, K.A. Maasch, The transition from arc volcanism to exhumation, weathering of young Ca, Mg, and Sr silicates, and CO_2 drawdown, in: T.J. Crowley, K.C. Burke (Eds.), Tectonic Boundary Conditions for Climate Reconstructions, Oxford, London, 1997, in press.

[22] C.R. German, R. Mills, A.P. Fleer, M.P. Bacon, N.C. Higgs, H. Elderfield, J. Thomson, A geochemical study of metalliferous sediment from the TAG hydrothermal mound, 25º08′N, MAR, J. Geophys. Res. 98 (1993) 9683–9692.

[23] M.R. Palmer, K.K. Falkner, K.K. Turekian, S.E. Calvert, Sources of osmium isotopes in manganese nodules, Geochim. Cosmochim. Acta 52 (1988) 1197–1202.

[24] G. Ravizza, G.M. McMurtry, Osmium isotopic variations in metalliferous sediments from the East Pacific Rise and the Bauer Basin, Geochim. Cosmochim. Acta 57 (1993) 4301–4310.

[25] G. Ravizza, C.E. Martin, C.R. German, G. Thompson, Os isotopes as tracers in seafloor hydrothermal systems: metalliferous deposits from the TAG hydrothermal area, 26ºN Mid-Atlantic Ridge, Earth Planet. Sci. Lett. 138 (1996) 105–119.

[26] K.W. Burton, J. Birck, C.J. Allègre, F. von Blanckenburg, R.K. O'Nions, J.R. Hein, Variations in the Osmium Iso-

tope Ratio of Seawater, Proc. 1996 Goldschmidt Conf., Heidelberg, J. Conf. Abstr. 1 (1996).
[27] M. Leinen, Shipboard Scientific Party, Site 598, Init. Rep. DSDP 92 (1986) 97–116.
[28] K. Hsü, Shipboard Scientific Party, Site 521, Init. Rep. DSDP 73 (1984) 137–186.
[29] E.L. Hoffman, A.J. Naldrett, J.C. Van Loon, R.G.V. Hancock, A. Mason, The determination of all the platinum group elements and gold in rocks and ore by neutron activation analysis after preconcentration by a nickel sulfide fire-assay technique for large samples, Anal. Chim. Acta 102 (1978) 157–166.
[30] L.C. Reisberg, C.J. Allègre, J.M. Luck, The Re–Os systematics of the Rhonda Ultramafic Complex of southern Spain, Earth Planet. Sci. Lett. 105 (1991) 196–213.
[31] E. Hauri, S.R. Hart, Re–Os isotope systematics of HIMU and EMII oceanic island basalts from the South Pacific Ocean, Earth Planet. Sci. Lett. 114 (1992) 353–371.
[32] N.J. Shackleton, M.A. Hall, A. Boersma, Oxygen and carbon isotope data from Leg 74 foraminifers, Init. Rep. DSDP 74 (1984) 599–612.
[33] L. Tauxe, P. Tucker, N.P. Petersen, J.L. LaBrecque, Magnetostratigraphy of Leg 73 sediments, Init. Rep. DSDP 73 609–622.
[34] S.F. Percival Jr., Late Cretaceous to Pleistocene calcareous nannofossils from the South Atlantic, Init. Rep. DSDP 73 391–424.
[35] R.Z. Poore, Middle Eocene through Quaternary planktonic foraminifers from the souther Angola basin, Init. Rep. DSDP 73 429–448.
[36] S. Knuttel, Calcareous nannofossil biostratigraphy of the central east Pacific, Deep Sea Drilling Project Leg 92: Evidence for downslope transport of sediments, Init. Rep. DSDP 92 (1986) 255–290.
[37] K. Romine, Planktonic foraminifers from Oligocene to Pleistocene sediments, Deep Sea Drilling Project Leg 92, Init. Rep. DSDP 92 (1986) 291–298.
[38] W.A. Berggren, K.V. Kent, C.C. Swisher III, M.P. Aubry, A revised Cenozoic geochronology and chronostratigraphy, in: W.A. Berggren, D.V. Kent, J. Hardenbol (Eds.), Geochronology, Time Scales, and Global Stratigraphic correlations: A Unified Temporal Framework for a Historical Geology, Soc. Econ. Paleontol. Mineral. Spec. Publ. 54 (1995) 129–212.
[39] W.H. Blow, Late middle Eocene to Recent planktonic foraminiferal biostratigraphy, First International Conference Planktonic Microfossils 1, 1969, pp. 199–421.
[40] K.G. Miller, J.D. Wright, R.G. Fairbanks, Unlocking the icehouse: Oligocene–Miocene oxygen isotopes, eustasy, and margin erosion, J. Geophys. Res. 96 (1991) 6829–6848.
[41] J.D. Wright, K.G. Miller, R.G. Fairbanks, Early and middle Miocene stable isotopes: Implications for deepwater circulation and climate, Paleoceanography 7 (1992) 357–389.
[42] F. Woodruff, S.M. Savin, Mid-Miocene isotope stratigraphy in the deep sea: High-resolution correlations, paleoclimatic cycles, and sediment preservation, Paleoceanography 6 (1991) 755–806.
[43] J.D. Wright, K.G. Miller, Control of North Atlantic Deep Water circulation by the Greenland–Scotia Ridge, Paleoceanography 11 (1996) 157–170.
[44] B.K. Esser, K.K. Turekian, The osmium isotopic composition of the continental crust, Geochim. Cosmochim. Acta 57 (1993) 3093–3104.
[45] W.J. Pegram, B.K. Esser, S. Krishnaswami, K.K. Turekian, The isotopic composition of leachable osmium from river sediments, Earth Planet. Sci. Lett. 128 (1994) 591–599.
[46] G. Ravizza, K.K. Turekian, Application of the ^{187}Re–^{187}Os system to black shale geochronometry, Geochim. Cosmochim. Acta 53 (1989) 3257–3262.
[47] G. Ravizza, K.K. Turekian, B.J. Hay, The geochemistry of rhenium and osmium in recent sediments from the Black Sea, Geochim. Cosmochim. Acta 55 (1991) 3741–3752.
[48] N.J. Shackleton, M.A. Hall, Stable isotope records in bulk sediments (Leg 138), Proc. ODP, Sci. Results 138 (1995) 797–805.
[49] N.J. Shackleton, M.A. Hall, The Late Miocene stable isotope record, Site 926, Proc. ODP, Sci. Results 154, in press.
[50] N.J. Shackleton, The carbon isotope record of the Cenozoic: History of organic carbon burial and of oxygen in the ocean and atmosphere, in: J. Brooks, A.J. Fleet (Eds.), Marine Petroleum Source Rocks, Blackwell, London, 1987, pp. 423–434.
[51] L.A. Derry, C. France-Lanord, Neogene growth of the sedimentary organic carbon reservoir, Paleoceanography 11 (1996) 267–275.
[52] G. Ravizza, B.K. Esser, A possible link between the seawater osmium isotope record and weathering of ancient sedimentary organic matter, Chem. Geol. 107 (1993) 255–258.
[53] J.I. Hedges, R.G. Keil, Sedimentary organic matter preservation: an assessment and speculative synthesis, Mar. Chem. 49 (1995) 81–115.
[54] M.E. Raymo, The Himalayas, organic carbon burial, and climate in the Miocene, Paleoceanography 9 (1994) 399–404.
[55] S.J. Goldstein, S.B. Jacobsen, The Nd and Sr isotopic systematics of river-water dissolved material: implications for the sources of Nd and Sr in seawater, Chem. Geol. 66 (1987) 245–272.
[56] S. Krishnaswami, J.R. Trivedi, M.M. Sarin, R. Ramesh, K.K. Sharma, Strontium isotopes and rubidium in the Ganga–Brahmaputra river system: Weathering in the Himalaya, fluxes to the Bay of Bengal and contributions to the evolution of oceanic ^{87}Sr/^{86}Sr, Earth Planet. Sci. Lett. 109 (1992) 243–253.
[57] J.M. Edmond, Himalayan tectonics, weathering processes, and the strontium isotope record in marine limestones, Science 258 (1992) 1594–1597.
[58] J.D. Blum, Y. Erel, A silicate weathering mechanism linking increase in marine ^{87}Sr/^{86}Sr with global glaciation, Nature 373 (1995) 415–418.
[59] J. Quade, L. Roe, P.G. DeCelles, T.P. Ojha, The Late

Neogene $^{87}Sr/^{86}Sr$ record of lowland Himalayan rivers, Science 276 (1997) 1828–1831.
[60] R.B. Sorkhabi, E. Stump, Rise of the Himalaya: A geochronologic approach, Geol. Soc. Am. Today 3 (1993) 86–92.
[61] W. Hamilton, Tectonics of the Indonesian Region, USGS Prof. Pap. 1078 (1979) 345 pp.
[62] T.C.W. Wolf-Welling, M. Cremer, S. O'Connell, A. Winkler, J. Thiede, Cenozoic Arctic gateway paleoclimate variability: Indications from changes in coarse-fraction composition, Proc. ODP, Sci. Results 151 (1996) 515–568.
[63] D. Colodner, J. Sachs, G. Ravizza, K.K. Turekian, J. Edmond, E. Boyle, The geochemical cycle of rhenium: A reconnaissance, Earth Planet. Sci. Lett. 117 (1993) 205–221.
[64] R. Oxburgh, N.J. Shackleton, Pleistocene variations in the osmium isotopic composition of sea water as indication of controls on continental weathering processes, Proc. 1996 Goldschmidt Conf., Heidelberg, J. Conf. Abst. 1 (1996) 447.